

# PHYSICAL REVIEW B

## CONDENSED MATTER

THIRD SERIES, VOLUME 45, NUMBER 6

1 FEBRUARY 1992-II

### Formation energy and lattice relaxation for point defects in Li and Al

R. Benedek and L. H. Yang\*

*Materials Science Division, Argonne National Laboratory, Argonne, Illinois 60439*

C. Woodward

*Universal Energy Systems, Dayton, Ohio 45432*

B. I. Min

*Department of Physics, Pohang Institute of Science and Technology, Pohang 680, Korea*

(Received 17 June 1991)

Calculations were performed for both a vacancy and an Al solute atom in bcc Li and for a vacancy in fcc Al. The purpose of this work was (i) to test optimization algorithms that allow a unified determination of ground-state electronic structure and lattice relaxation, and (ii) to compare calculated properties with experiment and with previous pair-potential simulations. 16- and 54-site supercells were employed in the Li-host calculations and a 32-site supercell was employed for the Al vacancy. The self-consistent Kohn-Sham orbitals, expanded in a plane-wave basis, were obtained using the modified steepest-descents algorithm of Williams and Soler and the band-by-band iteration method of Teter, Payne, and Allan. Electron-ion interactions were represented by generalized norm-conserving pseudopotentials cast in separable form. The relative performance of the two optimization algorithms is discussed. The equilibrium lattice relaxation was calculated by the Newton-Raphson method, with the Hessian matrix determined from numerical derivatives of the Hellman-Feynman forces. Calculated vacancy-formation energies are in excellent agreement with experiment.

#### I. INTRODUCTION

The local-density approximation (LDA) of density-functional theory has proven a robust framework for the calculation of cohesive properties of condensed matter.<sup>1</sup> The success of the LDA has spurred a search for numerical algorithms suitable for "large cells" that would enable molecular-dynamics simulations or structural-relaxation calculations with Hellmann-Feynman forces calculated at the LDA level. A breakthrough was achieved by Car and Parrinello,<sup>2</sup> who introduced iterative techniques that employ the total-energy gradient (with respect to Kohn-Sham orbitals), in conjunction with a plane-wave basis set and norm-conserving ionic pseudopotentials. Two insights that emerged from their work are (i) the computational efficiency of fast Fourier transformation in the evaluation of the gradient, and (ii) the efficacy of approximate Hellmann-Feynman forces computed in a plane-wave basis for molecular-dynamics or structural-relaxation calculation. Although the application (of energy-gradient methods) to molecular-dynamics simulation<sup>2</sup> has received the most attention, complementary techniques are also quite effective for structural-relaxation calculations, the focus of the present paper.

With these techniques, structural relaxation, e.g., for crystalline defects, disordered alloys, amorphous systems, and complex crystals, can be calculated at the LDA level, without resorting to arbitrary atomic-force models. In structural studies, local-optimization methods, such as the modified steepest descents<sup>3,4</sup> (MSD) and conjugate gradients<sup>5-7</sup> (CG), are more efficient than the Lagrangian scheme of Car and Parrinello for the calculation of ground-state Kohn-Sham orbitals.

As an initial application of gradient-based plane-wave optimization methods to structural relaxation in metallic systems, we consider substitutional point defects. The relaxation induced by vacancies and solute atoms is qualitatively known from force-model simulations, which provide a useful benchmark. Specifically, we treat the formation energy and defect-induced lattice relaxation for vacancies and Al solute atoms in Li (Refs. 8 and 9) and for a vacancy in Al, using the MSD (Ref. 4) and band-by-band<sup>6</sup> methods. The present work extends the band-by-band scheme of Ref. 6 to metallic systems.<sup>10</sup> Properties of monovacancies in Li have previously been studied by molecular-dynamics simulations with *ab initio* pair potentials<sup>11</sup> and with cluster electronic-structure calculations.<sup>12</sup> Several pseudopotential<sup>7,13,14</sup> and nonpseudopotential

linearized augmented-plane-wave<sup>15</sup> (LAPW) calculations have been reported for a vacancy in Al; lattice relaxation was included only in the last of these.

Section II outlines the optimization methods employed in the electronic-structure calculations. In Sec. III, the lattice-relaxation procedure is described. Section IV describes the numerical results for the lattice relaxation and the vacancy formation energy. Some implications of the present results are discussed in Sec. V.

## II. ELECTRONIC STRUCTURE METHOD

### A. Algorithms

An implementation of the MSD algorithm of Williams and Soler<sup>3</sup> based on a plane-wave basis set and norm-conserving pseudopotentials has been described in earlier work<sup>4</sup> (see also Ref. 16). The MSD algorithm incorporates the diagonal elements of the Hessian matrix, in contrast to classical SD, which employs only gradient information. This modification does accelerate convergence at least in the early iterations, although SD was found to yield better asymptotic convergence than MSD in some test calculations.<sup>5,6</sup> As Stich *et al.*<sup>5</sup> observe, the diagonal-dominance assumption in the MSD method becomes questionable for large unit cells. The CG method, on the other hand, is not affected by the sparsity of the Hessian, which makes it less subject to instability than MSD in large unit-cell applications. In the CG implementations described in Refs. 5 and 7 (as in the MSD treatment of Ref. 4), all orbitals for a given  $\mathbf{k}$  point are updated simultaneously, and the variation of the electron potential along the line-minimization path is neglected. Teter *et al.*,<sup>6</sup> noting the tendency of this procedure to overshoot, suggest an alternative CG algorithm based on a band-by-band optimization (we refer to this as BB), in which the line minimization can be performed essentially exactly, at least in insulating systems. Another virtue of the BB is its preconditioned form, helpful for treating large basis sets.

We have applied in the present work both the simplest (MSD) and the most elaborate (BB) of the above-mentioned optimization strategies to metallic systems. In both treatments, zone integrations were performed by special  $\mathbf{k}$ -point sampling using the Gaussian-broadening scheme. In treating metals, some excited-state orbitals as well as the occupied orbitals must be calculated; in the 54-site Li-cell calculations, 48 orbitals were treated and, in the 32-site Al cell, 60 orbitals were included. The BB line minimization for orbitals with small weight (less than  $10^{-3}$ , say) was performed on the orbital expectation value rather than the total energy. After each iteration of the MSD method (or each full pass through the bands for a given  $\mathbf{k}$  point in the BB method), a "subspace diagonalization" is performed to obtain an updated Fermi energy and set of weighting factors.

An analytical relation for  $d^2E/d\theta^2$  (Ref. 17) (in the notation of Ref. 6), was employed to improve the numerical precision of the BB line minimization. The BB line minimization is not exact in the case of metals, since the contributions to  $E(\theta)$  that correspond to changes in band

occupancy  $f_m(df/d\theta \neq 0)$  are neglected. The stability and convergence of the BB method were nevertheless found satisfactory in applications to metallic systems, as described below.

Generalized norm-conserving pseudopotentials<sup>18</sup> were constructed based on neutral-atom reference configurations with core radii  $r_l = 1.0, 1.1,$  and  $1.2$  a.u. for Li and  $r_l = 1.21, 1.55,$  and  $1.55$  a.u. for Al  $s, p,$  and  $d$  waves, respectively, and cast in the computationally efficient Kleinman-Bylander form.<sup>19</sup> Equilibrium lattice constants  $a = 6.20$  a.u. (7.52 a.u.) were obtained for Li (Al), respectively [experimental values are 6.59 a.u. (7.59 a.u.)] based on these potentials. The discrepancy between theory and experiment is considerably larger for Li than for Al, consistent with our earlier experience.<sup>4</sup> This discrepancy is only partly due to the pseudopotential construction; APW calculations for Li,<sup>20</sup> for example, yield  $a = 6.37$  a.u., still well below experiment.<sup>21</sup>

In the MSD calculations for  $L/a = 2$  and 3, charge-density mixing is required to avoid charge-sloshing instabilities. Thus, the charge-density distribution following subspace diagonalization is mixed (using the scheme introduced by Kerker<sup>23(a)</sup>) with the previous charge density to determine an electron potential.<sup>23(b)</sup> In the BB calculations, no charge-density mixing was found necessary to ensure stability for  $L/a = 1$  and 2, but mixing was required for  $L/a = 3$ . The BB calculations for the Al supercell with  $L/a = 2$  did not require mixing for stabilization. The initial-state orbitals (to start the iterative process) were either randomly generated or obtained by diagonalization of a small matrix.

### B. Convergence of optimization algorithms

The occupation-weighted residual norm,<sup>4</sup> where the residual is defined as  $(H_{KS} - \epsilon_i)\psi_i$ , provides a useful measure of convergence. A comparison of results obtained with the MSD and the BB algorithms for Li cells of different sizes is shown in Fig. 1. A marked deterioration in convergence rate was observed for the larger cells in the case of the MSD algorithm. Thus, although satisfac-

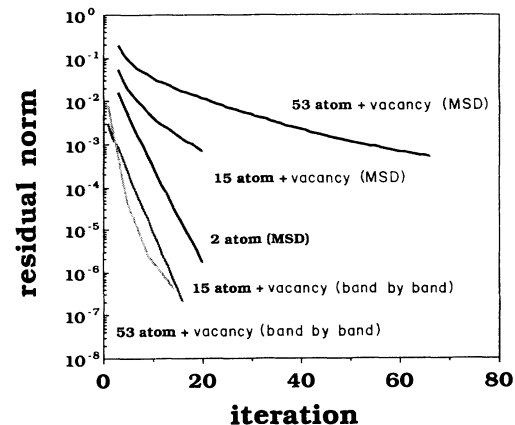


FIG. 1. Residual norm for calculations on Li cells based on the MSD and band-by-band algorithms.

tory convergence was obtained for  $L/a = 3$  in about 150 iterations, the convergence rate was considerably slower than for  $L/a = 2$ , and the next largest cell,  $L/a = 4$ , would probably require more than an order of magnitude larger number of iterations to converge. The results for the BB algorithm were based on one line minimization per band for each full pass through the bands. Although there is greater numerical effort in each iteration of the BB than in the MSD algorithm (perhaps a factor of 2), the overall performance of BB was vastly superior to MSD. Most important is that the convergence of the BB algorithm did not degrade significantly in going from  $L/a = 2$  to 3.

### C. Basis-set size and k-point sampling

The Li calculations were performed for simple-cubic supercells with  $L/a = 1, 2$  and 3, where  $a$  is the lattice constant and  $L$  is the supercell dimension, which correspond to 2, 16, and 54 sites. A basis-set cutoff of 10 Ry (3400 plane waves for the  $L/a = 3$  cell) was employed, similar to values chosen by Pawellek *et al.*<sup>9</sup> We used a single special  $\mathbf{k}$  point in the 54-site calculations, following the example of Hafner and Payne in their liquid-metal calculation for cells of comparable size.<sup>22</sup> Pawellek *et al.*<sup>9</sup> found a 12% reduction in the (relaxed) Li-vacancy formation energy (cf. Sec. IV B) in going from one to four  $\mathbf{k}$  points. Their calculations were based on a Gaussian broadening about three times smaller than our choice of  $\sigma = 0.05$  Ry, however, which might increase sensitivity to  $\mathbf{k}$ -point sampling. (6, 100)  $\mathbf{k}$  points were used in the (16, 2)-site calculations.

The Al-vacancy calculations were made for a simple-cubic supercell with  $L/a = 2$  (32 sites), and a cutoff energy of 22.5 Ry. Four special  $\mathbf{k}$  points were used with a broadening  $\sigma = 0.05$  Ry. In LAPW calculations, Mehl and Klein<sup>15</sup> found unrelaxed vacancy-formation energies increased about 10% in going from 10 to 110  $\mathbf{k}$  points; their (Fermi-function) broadening, however, was much smaller than ours.

The present choice of  $\mathbf{k}$ -point sets and broadening parameters are thought to provide reasonable precision at a moderate cost in the applications considered in this paper. Based on the experience in Refs. 9 and 15, one might estimate the  $\mathbf{k}$ -point sampling error in the present formation-energy calculations to be of order 10–15%.

## III. LATTICE RELAXATION METHOD

Although structural relaxation can, in principle, be calculated with the electronic and ionic degrees of freedom treated on the same footing<sup>4</sup> (in the spirit of Car-Parrinello dynamics,<sup>2</sup> it is more expedient to treat them separately, in order to minimize problems of overshoot and electronic-charge sloshing. In the present work, we regard the ionic coordinates as explicit variables and the electronic coordinates (Kohn-Sham orbital coefficients) as implicit variables that are constrained to lie on the Born-Oppenheimer surface. Minimization of the adiabatic energy function  $E[\mathbf{R}(l)]$ , with respect to the ionic configuration  $\mathbf{R}(l)$ , where  $l$  is the ion index, involves a

relatively small number of ionic degrees of freedom, and the rapidly convergent Newton-Raphson method is therefore feasible. The Newton-Raphson relaxation step

$$\mathbf{u} = \underline{\Phi}^{-1} \mathbf{F} \quad (1)$$

requires the first two derivatives,

$$\mathbf{F}(l) = -\partial E / \partial \mathbf{R}(l), \quad (2)$$

$$\Phi(l, l') = \partial^2 E / \partial \mathbf{R}(l) \partial \mathbf{R}(l'), \quad (3)$$

of the adiabatic energy function. In the case of the 54-site bcc cell, Eq. (1) can be expressed in terms of reduced variables (vectors  $\mathbf{F}$  and matrix  $\underline{\Phi}$ ) of dimension 6, the numbers of independent ionic degrees of freedom for a point-defect relaxation field with cubic symmetry<sup>24</sup> for a cell with  $L/a = 3$ . Since each of the six symmetry shells of atoms surrounding a central point defect has a single degree of freedom,<sup>25</sup> the index  $l$  can therefore be reinterpreted as a shell index in the reduced equations. Numerical values of the reduced force  $\mathbf{F}$  are obtained directly from the Hellmann-Feynman forces.<sup>26</sup> The elements of the reduced-force-constant matrix  $\underline{\Phi}$  were obtained by taking finite differences between Hellmann-Feynman forces for configurations that differ by a small displacement of a given shell of atoms from unrelaxed positions;<sup>27</sup> values of  $\Phi(l, l')$  obtained from displacing shells  $l$  and  $l'$  separately were averaged. Using the displacements obtained from Eq. (1), the relaxed atomic coordinates are given by  $\mathbf{R}(l) = \mathbf{R}_0(l) + \mathbf{u}(l)$ , where  $\mathbf{R}_0(l)$  represent the unrelaxed lattice sites. The self-consistent electronic structure and Hellmann-Feynman forces corresponding to the atomic coordinates were then calculated. The Hellmann-Feynman forces for the relaxed configuration show nonzero (but small) values as a result of (i) anharmonicity, and (ii) residual numerical inaccuracy in  $\mathbf{F}$  and  $\underline{\Phi}$ . If desired, the whole process involving Eqs. (1)–(3) could be iterated, or (as done in this work) further small adjustments in the configuration can be made “by hand,” using the Hellmann-Feynman forces for guidance. The first Newton-Raphson relaxation step, however, already gives a quite accurate estimate of the equilibrium displacements and the relaxation energy.

Since the relaxation surrounding a point defect in a supercell is constrained by the periodic boundary conditions, it is important to use a sufficiently large cell to model an isolated defect. The 53-atom cell provides an accurate estimate of the relaxation energy for a vacancy in a bcc crystal, whereas the 31-atom fcc cell is large enough to account for most of the vacancy relaxation energy in that structure.

## IV. RESULTS

### A. Lattice relaxation

We discuss first the 54-site Li cell. The displacements of the six coordination shells surrounding either a vacancy or an Al solute atom are plotted in Fig. 2, in half-lattice constant units. The results for the vacancy are in close agreement with those given in Ref. 9. A characteristic feature for vacancies is that the first two neigh-

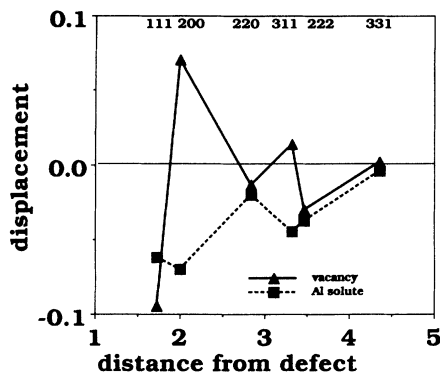


FIG. 2. Calculated displacements of six neighbor shells surrounding vacancy (triangles) and Al solute atom (squares) in 54-site Li supercell. Units of ordinate and abscissa scales:  $a/2$  (half-lattice constants). Indices of the shells are indicated at the top.

neighbors have displacements of opposite sign. The displacements of the first two neighbors are roughly proportional to the Hellmann-Feynman forces (in the unrelaxed lattice), as illustrated in Fig. 3, and the sign change in the displacements and in the Hellmann-Feynman forces have the same physical origin. This sign change occurs in pairwise-force model simulations for a vacancy in the bcc structure as a consequence of the minimum in the interionic potential between the first- and second-neighbor separations;<sup>28</sup> see, e.g., the potentials of Dagens *et al.*<sup>29</sup> The calculated lattice relaxation for a vacancy in Li (for those shells within the supercell boundary) is compared with pair-potential simulations<sup>30</sup> for Na (the range of results for which are indicated by the error bars) in Fig. 4. We observe that the relaxation in Li follows a very similar pattern to previous results for Na. In the case of an Al solute in Li, we see in Fig. 2 that the displacements of both the first two neighbors are inward, with no sign change. This result indicates that the effective Al-Li potential in this system is more attractive than the Li-Li host potential at the second-nearest-neighbor separation.

After the vacancy lattice relaxation was determined,

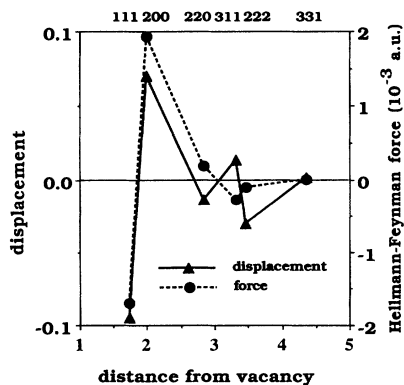


FIG. 3. Equilibrium displacements (triangles) and (unrelaxed) Hellmann-Feynman forces (circles) for shells surrounding vacancy in 54-site Li cell. Units of displacements and distance from vacancy:  $a/2$  (half-lattice constants).

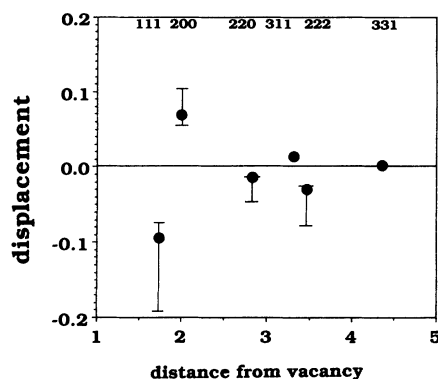


FIG. 4. Displacements calculated for 54-site Li cell with vacancy (solid circle) and range of calculated displacements from pair-potential simulations for Na (Ref. 30) (bars). Units of ordinate and abscissa scales:  $a/2$  (half-lattice constants).

the cell lattice parameter was varied to determine the equilibrium atomic volume. From this result, a vacancy-formation volume of 0.63 atomic volumes was obtained, slightly larger than the values 0.58 and 0.52 given in Ref. 9.

In the case of a vacancy in Al, the Hellmann-Feynman force on the nearest-neighbor shell was found to vary essentially linearly with displacement, and the zero crossing (equilibrium) occurs for an inward relaxation of 0.09 a.u. ( $0.012a$ ). A slightly smaller value for the nearest-neighbor displacement, 0.065 a.u., was obtained by Mehl and Klein.<sup>15</sup> Our results are also in reasonable agreement with those obtained in pair-potential calculations.<sup>31</sup> The determination of more distant-neighbor relaxations would require a larger supercell than employed here. Judging from the work of Gillan,<sup>7</sup> however, the effect of the relaxation of the second and more distant shells on the formation energy (discussed below) is a most a few hundredths of an eV.

The effect of lattice relaxation on the charge distribution is illustrated in Fig. 5, which shows charge-density contours in a  $[110]$  plane containing the vacancy (located at the center), in the 53-atom Li cell. The first panel refers to the unrelaxed cell and illustrates that the disturbance in the charge density is largely confined to the region of the first two neighbor shells [the six atoms nearest the vacancy in the figure include two members of the (200) shell and four members of the (111) shell]. The second panel corresponds to the relaxed lattice, in which the disturbance extends slightly beyond the second-neighbor shell. The redistribution of electronic charge density as a result of relaxation can be summarized as follows. The charge density at the center of the vacancy increases from  $3.0 \times 10^{-3}$  to  $3.6 \times 10^{-3}$  a.u.; for comparison, the mean conduction electron density is  $8.4 \times 10^{-3}$  a.u. The charge density between the (111) and (222) shells decreases as a result of the increased interatomic separation [note the lighter contrast in Fig. 5(b) as compared to Fig. 5(a)], whereas the charge density between the (200) and (400) shells increases (as indicated by darker contrast) due to the decrease in the corresponding interatomic separation.

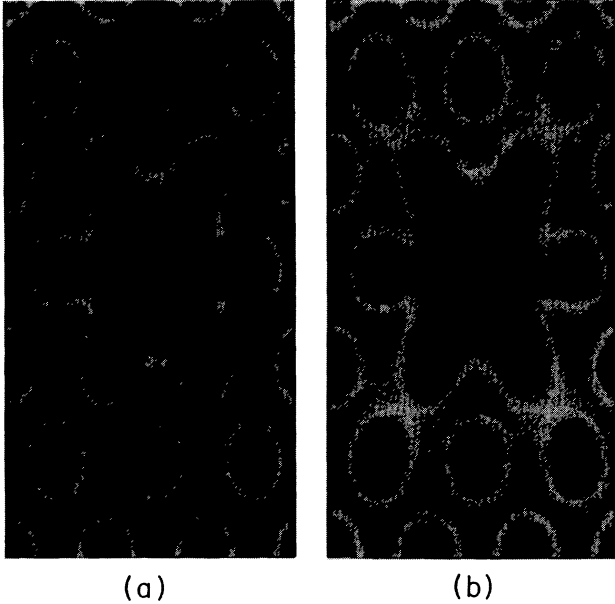


FIG. 5. Charge-density contours in 110 plane of 54-site Li cell containing vacancy. (a) and (b) correspond to the unrelaxed and relaxed lattices, respectively. The short axis corresponds to the [001] direction and the long axis to the [110] direction. The scales are unequal, which make the atoms appear elliptical.

### B. Vacancy-formation energy

The vacancy-formation energy is obtained from supercell calculations as the difference

$$E_{1v} = E(N-1, V') - [(N-1)/N]E(N, V) \quad (4)$$

between the energy of the defect supercell with  $N-1$  atoms and that of the perfect crystal scaled to the same number of atoms. If  $V/N$  is the zero-pressure atomic volume of the perfect crystal, then the difference between the vacancy-formation energy at constant pressure (measured experimentally) and constant volume is small because of the stationarity of the energy. Results for the calculated vacancy-formation energies are listed in Table I. The unrelaxed values correspond to the perfect lattice, and the relaxed values are based on the lattice relaxation calculated as described in Sec. III. In the case of Li, two supercell sizes are shown. The relaxation energy for the 53-atom Li cell (0.09 eV) is expected to be converged since neighbors beyond the second cell contribute little; in molecular-dynamics simulations for Li with  $L/a = 4$ , a relaxation energy of 0.07 eV was obtained.<sup>32</sup>

The experimental value of  $E_{1v}$  for Li determined by di-

latometry,<sup>33</sup> 0.34 eV, is considerably smaller than that obtained from the difference between self-diffusion activation energy and migration energy,<sup>34</sup> 0.48 eV. We favor the latter value since the former would imply a much larger migration energy for Li than for other alkalis, which seems unlikely. The value of 0.48 eV is in reasonable agreement with our theoretical estimate for the 54-site cell, 0.57 eV. The present results for formation energy of Li are in excellent overall agreement with those of Ref. 9 in spite of differences in the pseudopotentials employed.

The calculated formation energy for Al, including relaxation of the first-neighbor shell, is 0.71 eV. As mentioned above, the relaxation energy associated with more distant shells would be small. The present result is in close agreement with the experimental values of 0.66 eV (Ref. 35) (positron annihilation spectroscopy) and 0.70 eV (Ref. 36) (quenching). A calculated value of 0.52 eV (in contrast to the present result of 0.78 eV) was obtained for the (unrelaxed) vacancy-formation energy of Al by Jansen and Klein,<sup>37</sup> based on a Hamann-Schlüter-Chiang pseudopotential<sup>38</sup> and a basis-set cutoff energy of 11 Ry. This is a larger discrepancy than we would have expected, and its origin is not presently clear.

## V. CONCLUSIONS

The MSD (Ref. 4) and BB (Ref. 6) algorithms have been tested in calculations for point defects in Li and Al. Both methods are feasible for the cell sizes treated here, but the BB shows superior convergence and scaling behavior and is therefore clearly preferable. We have demonstrated in the Li calculations a lattice-relaxation procedure based on the Newton-Raphson method, reminiscent of the method of lattice statics<sup>24</sup> that provides excellent convergence in only a single relaxation step. This method should become even more attractive with the implementation of linear response methods to obtain the Hessian matrix.<sup>27</sup> The calculated lattice relaxation for the vacancies in Li and Al are in reasonable agreement with previous results based on pair potentials.<sup>30,31</sup>

Although some questions remain, the calculated vacancy-formation energies for Li and Al appear to be in close agreement with experiment. This indicates that the present methodology, which involves a plane-wave expansion in a pseudopotential representation, is sufficiently precise and realistic to predict defect properties at least in simple metals. These results are in contrast to previous formation energy calculations based on pair potentials, which have often given unphysical values, particularly in the case of Al.<sup>39</sup> The present results, in conjunction with the recent studies of vacancies in transition metals by

TABLE I. Monovacancy formation energy (eV).

Element	$L/a$	$a$ (a.u.)	Unrelaxed	Theory		Experiment
				Relaxed		
Li	2	6.20	0.70	0.68		
Li	3	6.20	0.66	0.57	0.48 (Ref. 34), 0.34 (Ref. 33)	
Al	2	7.52	0.78	0.71	0.66 (Ref. 35), 0.70 (Ref. 36)	

Drittler *et al.*,<sup>40</sup> indicate that vacancy formation energies for most elemental metals can now be accurately calculated within the LDA framework.

#### ACKNOWLEDGMENTS

This work was supported by the U. S. Department of Energy under Contract No. W-31-109-ENG-38. It

benefited from an allocation of computer time at the National Energy Research Supercomputer Center at Lawrence Livermore National Laboratory. We are grateful to D. C. Allan for making available unpublished notes on the BB method, to E. Shirley for generating the Li pseudopotentials used in this work, and to D. Wolf for interesting discussions.

\*Present address: Lawrence Livermore National Laboratory, Physics/H Division, P. O. Box 808, Livermore, CA 94550.

<sup>1</sup>See, e.g., G. P. Srivastava and D. Weaire, *Adv. Phys.* **36**, 463 (1987).

<sup>2</sup>R. Car and M. Parrinello, *Phys. Rev. Lett.* **55**, 2471 (1985); **60**, 204 (1988).

<sup>3</sup>A. R. Williams and J. Soler, *Bull. Am. Phys. Soc.* **32**, 562 (1987).

<sup>4</sup>C. Woodward, B. I. Min, R. Benedek, and J. Garner, *Phys. Rev. B* **39**, 4853 (1989).

<sup>5</sup>I. Stich, R. Car, M. Parrinello, and S. Baroni, *Phys. Rev. B* **39**, 4997 (1989).

<sup>6</sup>M. P. Teter, M. C. Payne, and D. C. Allan, *Phys. Rev. B* **40**, 12 255 (1989).

<sup>7</sup>M. J. Gillan, *J. Phys.: Condens. Matter* **1**, 689 (1989).

<sup>8</sup>A preliminary report on the Li-vacancy calculations was presented earlier: R. Benedek, C. Woodward, and B. I. Min, *Bull. Am. Phys. Soc.* **35**, 573 (1990).

<sup>9</sup>A concurrent but independent study of the properties of a Li vacancy, along lines similar to those presented here, was performed by R. Pawellek, M. Faehle, C. Elsaesser, K.-M. Ho, and C.-T. Chan, *J. Phys.: Condens. Matter* **3**, 2451 (1991).

<sup>10</sup>An application of the CG method to dopant point-defect complexes in *a*-Si:H was recently performed by one of us. L. H. Yang, C. Y. Fong, and C. S. Nichols, *Phys. Rev. Lett.* **66**, 3373 (1991).

<sup>11</sup>G. Jacucci and R. Taylor, *J. Phys. F* **9**, 1489 (1979).

<sup>12</sup>M. R. Pederson, J. G. Harrison, and B. M. Klein, *Mater. Res. Soc. Symp. Proc.* **141**, 153 (1989).

<sup>13</sup>B. Chakraborty and R. W. Siegel, *Phys. Rev. B* **27**, 4535 (1983).

<sup>14</sup>R. W. Jansen and B. M. Klein, *J. Phys.: Condens. Matter* **1**, 8359 (1989).

<sup>15</sup>M. J. Mehl and B. M. Klein, *Physica B* **172**, 211 (1991).

<sup>16</sup>G. W. Fernando, G.-X. Qian, M. Weinert, and J. W. Davenport, *Phys. Rev. B* **40**, 7985 (1989).

<sup>17</sup>This refinement on the original treatment of Ref. 6 was suggested by D. C. Allan (private communication).

<sup>18</sup>D. R. Hamann, *Phys. Rev. B* **40**, 2980 (1989).

<sup>19</sup>L. Kleinman and D. M. Bylander, *Phys. Rev. Lett.* **48**, 1425 (1982).

<sup>20</sup>M. Sigalas, N. C. Bacalis, D. A. Papaconstantopoulos, M. J. Mehl, and A. C. Switendick, *Phys. Rev. B* **42**, 11 637 (1990); Jaejun Yu *et al.* (unpublished), obtained a similar value.

<sup>21</sup>Using a GNCP pseudopotential including the partial-core correction [S. Louie, S. Froyen and M. L. Cohen, *Phys. Rev. B* **26**, 1738 (1982)], we obtained a Li lattice constant close to the APW result. The effect of zero-point vibrations, not included in the above-mentioned results, increases the lattice constant by approximately 1% for Li. Application of the Perdew-Wang gradient correction to Li yielded a 1–2% increase in the calculated lattice constant [B. Barbiellini, E. G. Moroni, and T. Jarlborg, *J. Phys.: Condens. Matter* **2**, 7597 (1990)].

<sup>22</sup>J. Hafner and M. C. Payne, *J. Phys.: Condens. Matter* **2**, 221

(1990).

<sup>23</sup>(a) G. P. Kerker, *Phys. Rev. B* **23**, 3082 (1981); (b) The Kerker algorithm has previously been applied in the context of the band-by-band algorithm by D. M. Bylander, L. Kleinman, and S. Lee, *Phys. Rev. B* **42**, 1394 (1990). Our treatment differs from theirs in that we update the charge density both during the band-by-band optimization and after the subspace diagonalization.

<sup>24</sup>V. K. Tewary, *Adv. Phys.* **22**, 757 (1973).

<sup>25</sup>The [311] and [331] shells each have only a single relaxational degree of freedom since they lie on the cell boundary.

<sup>26</sup>Tests of Hellmann-Feynman force calculations, at least for perfect crystal distortions, are available in terms of experimentally determined Born-von Karmann force constants. Consider a radial breathing distortion  $\mathbf{u}(l) = \sqrt{3}\mathbf{R}(l)d/R(l)$  of the eight nearest neighbors to a central site in a perfect bcc crystal. In terms of Born-von Karmann force constants, the component Hellmann-Feynman forces  $F_x(l)/d = 8\alpha_1 + \alpha_2 + 6\beta_2 + 6\alpha_3 - \gamma_3 + 2\beta_3 + 8\alpha_4 + 16\beta_4 + 7\alpha_5$ . With the force constants of M. M. Beg and M. Nielsen [*Phys. Rev. B* **14**, 4266 (1976)], the right-hand side is equal to 2.18 ergs/cm<sup>2</sup>, whereas our Hellmann-Feynman force calculation for a distorted 54-atom Li supercell gave a value 2.25 ergs/cm<sup>2</sup>.

<sup>27</sup>Linear-response methods provide an alternative (most likely preferable) approach to obtain the second-derivative matrix. X. Gonze and J.-P. Vigneron, *Phys. Rev. B* **39**, 13 120 (1990); P. Giannozzi, S. di Gironcoli, P. Pavone, and S. Baroni, *ibid.* **43**, 7231 (1991).

<sup>28</sup>A potential minimum between the first two neighbors is a common feature for bcc crystals (Ref. 29), since it promotes the stability of that structure.

<sup>29</sup>L. Dagens, M. Rasolt, and R. Taylor, *Phys. Rev. B* **11**, 2726 (1975).

<sup>30</sup>P. S. Ho, *Phys. Rev. B* **3**, 4035 (1971).

<sup>31</sup>K. M. Miller and P. T. Heald, *Phys. Status Solidi B* **67**, 569 (1975).

<sup>32</sup>G. Jacucci and R. Taylor, *J. Phys. F* **9**, 1489 (1979).

<sup>33</sup>R. Feder, *Phys. Rev. B* **4**, 828 (1970).

<sup>34</sup>P. Ehrhart and H. Schultz, in *Numerical and Functional Relationships in Science and Technology*, edited by H. Ullmaier, Landolt-Börnstein New Series, Vol. III, Pt. 25, Chap. 2 (Springer-Verlag, Berlin, 1991); H. Schultz, *Mater. Sci. Eng.* **4**, 1 (1991).

<sup>35</sup>M. Fluss, L. C. Smedskjaer, M. K. Chason, D. G. Legnini, and R. W. Siegel, *Phys. Rev. B* **17**, 3444 (1978).

<sup>36</sup>J. Mundy, *Phys. Status Solidi B* **144**, 233 (1987).

<sup>37</sup>R. W. Jansen and B. M. Klein, *J. Phys.: Condens. Matter* **1**, 8359 (1989).

<sup>38</sup>D. Hamann, H. Schlüter, and C. Chiang, *Phys. Rev. Lett.* **43**, 1494 (1979).

<sup>39</sup>G. Jacucci, R. Taylor, A. Tenenbaum, and N. V. Doan, *J. Phys. F* **11**, 793 (1981).

<sup>40</sup>B. Drittler, M. Weinert, R. Zeller, and P. H. Dederichs, *Phys. Rev. B* **42**, 9336 (1990); (unpublished).

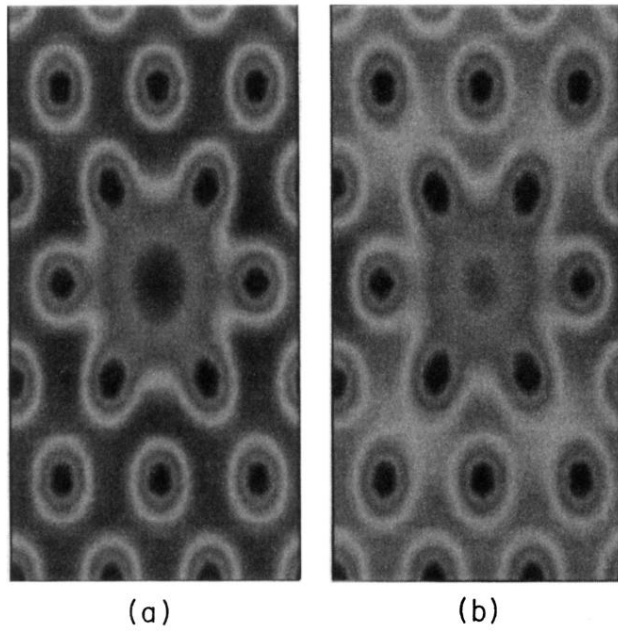


FIG. 5. Charge-density contours in 110 plane of 54-site Li cell containing vacancy. (a) and (b) correspond to the unrelaxed and relaxed lattices, respectively. The short axis corresponds to the  $[001]$  direction and the long axis to the  $[110]$  direction. The scales are unequal, which make the atoms appear elliptical.